

# Synthesis and electrochemical performance of thiophene containing conjugated microporous polymer derived sulfur-doped porous carbon

**Qingtang Zhang, Yan Meng and Qinqin Dai**

School of Petrochemical Engineering, Lanzhou University of Technology, Lanzhou, 730050, China  
zhqt137@163.com

**Abstract.** Sulfur-doped porous carbon (SPC) was obtained by pyrolyzing sulfur containing conjugated microporous polymer (SCMP). SPC was characterized by SEM, EDS, cyclic voltammetry and galvanostatic charge-discharge test. SEM results indicate that SPC are composed of sphere nanoparticles. EDS results imply that the carbon and sulfur elemental distribution of SPC is just like the shape of SPC and sulfur is uniformly distributed in SPC. The lithium storage capacity of SPC is up to  $536 \text{ mAh}\cdot\text{g}^{-1}$  at  $0.1 \text{ A}\cdot\text{g}^{-1}$ . In addition, the capacity cycled at  $0.6 \text{ A}\cdot\text{g}^{-1}$  for 300 cycles is as high as  $329 \text{ mAh}\cdot\text{g}^{-1}$ . Due to the S doping, SPC exhibits both high capacity and reliable cycling performance, making it a promising electrode material for LIBs.

## 1 Introduction

Lithium-ion batteries (LIBs) have been regarded as one of the most promising power sources owing to its remarkable advantages such as high power and energy density, long cycle life and environmental benign [1-3]. Porous carbons, as a kind of carbon-based anode materials, have been intensely investigated due to their intrinsic high specific capacity. In addition, the porous structure can provide materials with more lithium ions transportation paths and larger surface area for electrochemical reaction [4]. Sulfur doping has been seen as a pivotal strategy for enhancing electronic conductivity and storage sites of lithium, further improving lithium storage performance of porous carbon [5]. To date, a number of methods have been developed to prepare sulfur-doped carbon materials such as pyrolysis sulfonation [6], sulfate [7], and pyrolysis of sulfur-containing precursors such as thiourea [8] and bioresources [9].

Conjugated microporous polymer (CMP) is well known as rigid  $\pi$ -conjugated structure, tuned porous structures and excellent thermal and chemical stability. CMPs have a characteristic advantage of the structural flexibility that can be well tuned by changing reaction solvents, molecular structure, or chemical constitution of building blocks building the CMP network [10,11]. Interestingly, it can be realized by choosing sulfur-containing monomer to obtain sulfur-containing CMP (SCMP). In this study, SPC was prepared from SCMP, which is obtained through palladium-catalyzed Sonogashira-Hagihara crosscoupling condensation of 1,3,5-triethynylbenzene and 2,3,5-tribromothiophene. Then the structure and electrochemical properties of SPC is studied.

## 2 Experimental

### 2.1 Sample Preparation

1,3,5-triethynylbenzene was purchased from TCL. 2,3,5-tribromothiophene, copper(I) iodide and



Content from this work may be used under the terms of the [Creative Commons Attribution 3.0 licence](https://creativecommons.org/licenses/by/3.0/). Any further distribution of this work must maintain attribution to the author(s) and the title of the work, journal citation and DOI.

tetrakis (triphenyl-phosphine) palladium(0) were all purchased from J&K. All starting chemicals were used without any purification. 1,3,5-triethynylbenzene and 2,3,5-tribromothiophene were used to synthesize SCMP by Pd(0)/Cu(I) catalyzed Sonogashira-Hagihara cross-coupling polycondensation. 30 mg CuI, 100 mg tetrakis (triphenyl-phosphine) palladium(0), 1 mmol 2,3,5-Tribromothiophene and 1.5 mmol 1,3,5-triethynylbenzene were put into the mixture of 5 ml N,N-dimethylformamide (DMF) and 5 ml Et<sub>3</sub>N. The mixture solution was stirred constantly at 80 °C for 24 h under N<sub>2</sub> atmosphere. After the reaction was ending, the product was cooled to room temperature and the resulting SCMP was firstly filtered and washed with dichloromethane, acetone, water and methanol several times to remove unreacted or catalyst. Then, the obtained SCMP was purified by Soxhlet extraction with methanol for 72 h. Subsequently, SCMP was dried at 70 °C for 24 h. SCMP was directly calcined at 550 °C for 4 h under N<sub>2</sub> protection to obtain SPC.

## 2.2 Characterization

The morphologies of SPC were determined using scanning electron microscopy (SEM). Elemental composition analysis of SPC were recorded with energy-dispersive X-ray spectroscopy (EDS). The CR2032 coin-type cells were assembled to analyze the electrochemical performance of SPC. The electrodes were composed of 80% SPC, 10% super P, and 10% LA132 aqueous binder. Then the mixture was spread onto a copper foil. Finally, it was dried at 100 °C for 8 h in vacuum. The cells were assembled using lithium flake as counter electrode and 1 mol·L<sup>-1</sup>LiPF<sub>6</sub> in a mixture of ethylene carbonate/dimethyl carbonate/ethyl-methyl carbonate (1:1:1) as the electrolyte. The cells were charged-discharged in the voltage range of 0.00-3.00 V on a LAND CT2001A battery tester (Wuhan Lanbo Testing equipment co. LTD.). The cyclic voltammetry (CV) of the fresh cells were performed on a ZF100 electrochemical workstation (Shanghai Zhengfang Electronics Co., Ltd.) with different scan rates.

## 3 Results and Discussion

The SEM images and corresponding elemental distribution of SPC are shown in Figure. 1. As shown in Figure 1a, SPC are composed of some larger particles with smooth surface, some larger particle with rough surface area and numerous corresponding small particles. Observed from Figure 1b and c, these particles are all constituted by aggregated nanometer-sized spherical particles. Figure 1e and 1f indicate that the shape of carbon and sulfur elemental distribution. The carbon and sulfur elemental shapes are just like the particle shape of SPC shown in Figure 1d. These indicate that sulfur element is uniformly distributed with carbon element in the SPC.

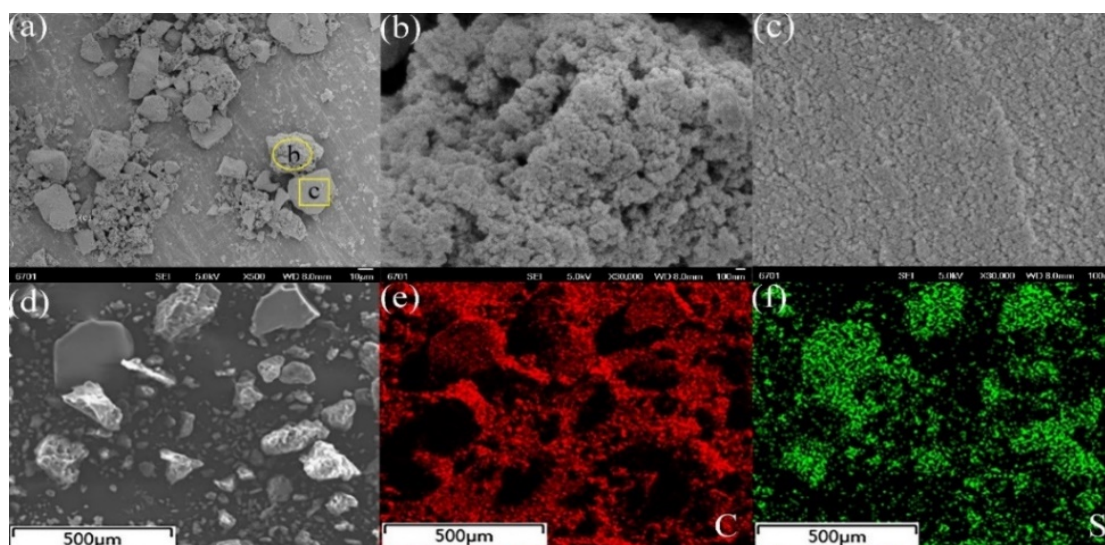


**Figure. 1** SEM images of SPC (a-c) and SEM-EDS mapping of images of (e) carbon and (f) sulfur for corresponding SEM images of SPC (d).

CV profiles were showed for the first (Figure 2a) and second (Figure 2b) cycles. SPC shows the electrochemical behaviors of typical carbonaceous materials. For the first CV scan in Figure 2a, SPC shows a broad cathodic peak at 0.2-1.7 V but disappears in subsequent cycles (Figure 2b), which is related to some irreversible electrochemical reactions and the formation of an SEI layer covered on the SPC surface. In addition, the sharp peak around 0 V is assigned to the insertion of lithium into the carbonaceous materials, as seen from Figure 2a and 2b. In the first and second anodic scan, the broad peak around 0.3 V is ascribed to the deintercalation of lithium from the carbon materials.

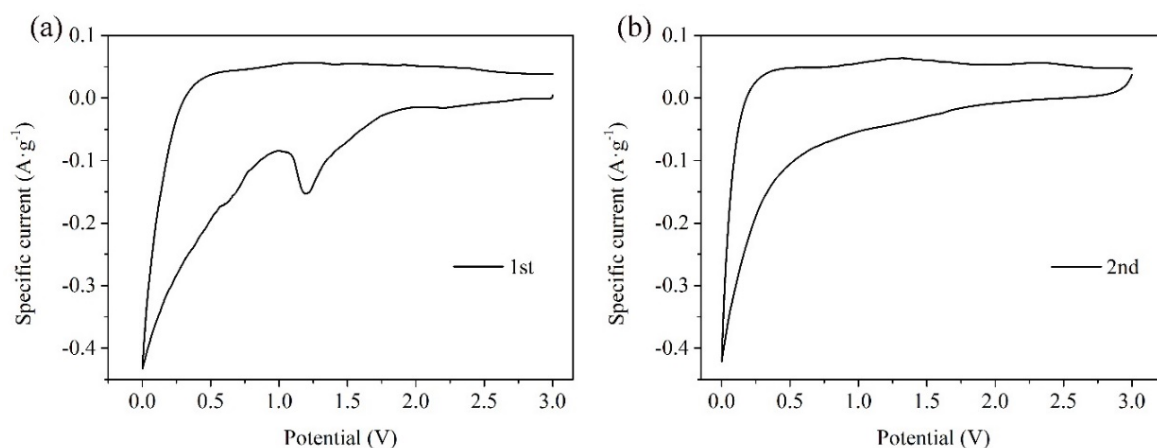


**Figure. 2** CV curves of at a scan rate of  $0.1 \text{ mV} \cdot \text{s}^{-1}$  (a) first cycle and (b) the second cycle.

Figure 3 show the charge-discharge curves of SPC in the first and fifth cycles. As shown in Figure 3a, the initial discharge capacity of SPC can reach  $1585.5 \text{ mAh} \cdot \text{g}^{-1}$ , and the initial charge capacity is  $653.8 \text{ mAh} \cdot \text{g}^{-1}$ . Therefore, the initial coulombic efficiency of SPC is only 41.2%. Low coulombic efficiency can be attributed to the formation of SEI layer and some irreversible reactions in the first cycle. In the fifth cycles (Figure 3b), the discharge and charge capacities of SPC are  $526.8 \text{ mAh} \cdot \text{g}^{-1}$  and  $504.1 \text{ mAh} \cdot \text{g}^{-1}$ , respectively. So, the SPC has a fifth coulombic efficiency of 95.7%. Therefore, coulombic efficiencies of SPC have been greatly increased at the fifth cycles.

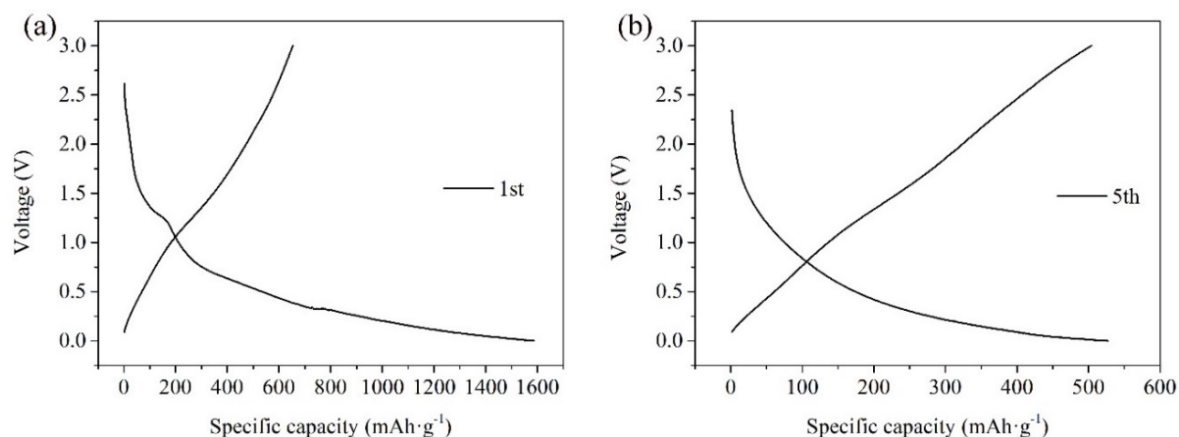


**Figure. 3** Charge-discharge curves (a) first cycle and (b) fifth cycle.

Figure 4a shows the rate performance of SPC. SPC delivers reversible capacity (third charge capacity at every current density) of 536, 361, 247, 169, 153 and 127  $\text{mAh} \cdot \text{g}^{-1}$  at the current density of 0.1, 0.2, 0.4, 0.8, 1.0 and 1.5  $\text{A} \cdot \text{g}^{-1}$ . And the attenuation of specific capacity is low in large current density of 1.5  $\text{A} \cdot \text{g}^{-1}$ . While restored at 0.1  $\text{A} \cdot \text{g}^{-1}$ , the reversible capacity of SPC can also maintain 428  $\text{mAh} \cdot \text{g}^{-1}$  without obvious capacity loss. Therefore, SPC as anode materials have good rate

performance. Figure 4b shows the cycling performance of SPC at a  $0.6 \text{ A}\cdot\text{g}^{-1}$  for 300 cycles. The second and 300th reversible capacity of SPC are  $222$  and  $329 \text{ mAh}\cdot\text{g}^{-1}$ . Thus, the capacity retention ratio of SPC is calculated to be 149%. This capacity-rise phenomenon can be derived from sulfur-doping generating defects in porous carbon materials, thus providing more active sites for Li insertion.

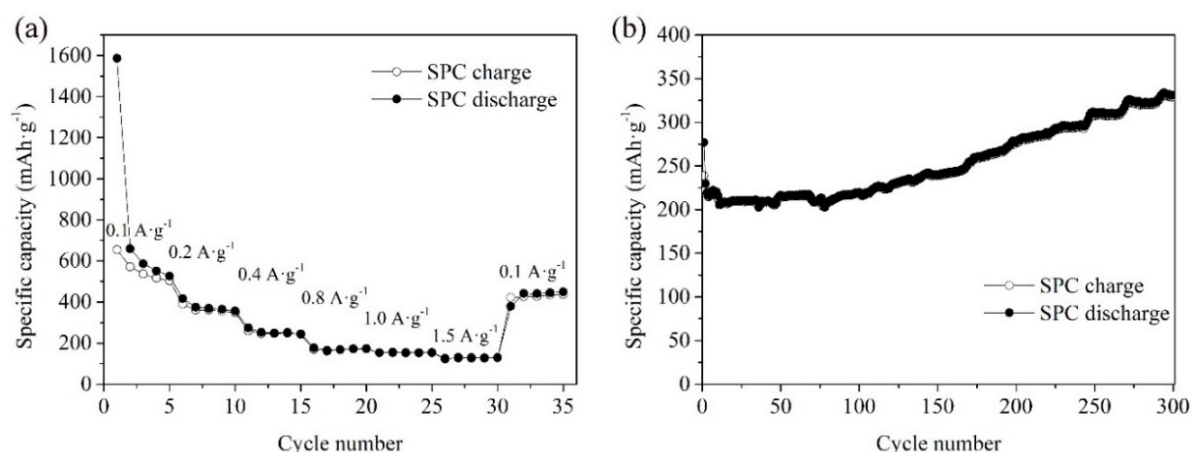


**Figure. 4** The rate performance of SPC at different current densities (a) and cycling performance of SPC at a current density of  $0.6 \text{ A}\cdot\text{g}^{-1}$  (b).

#### 4 Conclusions

SPC was obtained simply by pyrolyzing SCMP. SEM results indicate that SPC are composed of sphere nanoparticles. EDS results imply that the carbon and sulfur elemental distribution of SPC is just like the shape of SPC. Sulfur doping can enhance electronic conductivity and storage sites of lithium, thus improving lithium storage performance of porous carbon. Therefore, SPC shows excellent electrochemical performance. The reversible capacity is up to  $536 \text{ mAh}\cdot\text{g}^{-1}$  at  $0.1 \text{ A}\cdot\text{g}^{-1}$ . In addition, the capacity of SPC cycled at  $0.6 \text{ A}\cdot\text{g}^{-1}$  for 300 cycles is as high as  $329 \text{ mAh}\cdot\text{g}^{-1}$ .

#### Acknowledgements

This research was supported by the National Nature Science Foundation of China (No. 21466020).

#### References

- [1] Marom R, Amalraj S F, Leifer N, Jacob D and Aurbach D 2011 *Journal of Materials Chemistry* **21** 9938-54
- [2] Scrosati B, Hassoun J and Sun YK 2011 *Energy & Environmental Science* **4** 3287-95
- [3] Zhang Q T, Mei J T, Wang X M, Guo J H, Tang F L and Lu W J 2014 *Journal of Alloys and Compounds* **617** 326-331
- [4] Fu L J, Zhang T, Cao Q, Zhang H P and Wu Y P 2007 *Electrochemistry Communications* **9** 2140-44
- [5] Yan Y, Yin Y X, Xin S, Guo Y G and Wan L J 2012 *Chem Commun* **48** 10663-5
- [6] Sun Y H, Zhao J H, Wang J L, Tang N, Zhao R J, Zhang D D, Guan T T and Li K X 2017 *The Journal of Physical Chemistry C* **121** 10000-9
- [7] Ning G Q, Ma X L, Zhu X, Cao Y M, Sun Y Z, Qi C L, Fan Z J, Li Y F, Zhang X, Lan X Y and Gao J S 2014 *ACS Appl Mater Interfaces* **6** 15950-8
- [8] Jourshabani M, Shariatnia Z and Badieli A 2017 *Langmuir* **33** 7062-78
- [9] Lu M J, Yu W H, Shi J, Liu W, Chen S G, Wang X L and Wang H L 2017 *Electrochimica Acta* **251** 396-406
- [10] Chen Y F, Sun H X, Yang R X, Wang T T, Pei C J, Xiang Z T, Zhou Z Q, Liang W D, Li A and Deng W Q 2015 *Journal of Materials Chemistry A* **3** 87-91
- [11] Bao L L, Sun H X, Zhu Z Q, Liang W D, Mu P, Zang J K and Li A 2016 *Materials Letters* **178** 5-9